Effective surface impedance of polycrystals under anomalous skin effect conditions

Inna M. Kaganova
Institute of High Pressure Physics, Russian Academy of Sciences, 142092 Troitsk Moscow Region, Russia

Moisey I. Kaganov
7 Agassiz Avenue, Belmont, Massachusetts 02478

(Received 21 December 1999; revised manuscript received 24 April 2000; published 4 January 2001)

The effective impedance of strongly anisotropic polycrystals has been investigated under the conditions of extremely anomalous skin effect. We were interested in finding out how the value of the effective impedance depends on the geometry of the Fermi surface of a single crystal grain. The previously obtained nonperturbative solution based on the application of the impedance (the Leontovich) boundary conditions was used to calculate the effective impedance of a polycrystalline metal. Some model Fermi surfaces were examined. In the vicinity of the electronic topological transition the singularities of the effective impedance related to the change of the topology of the Fermi surface were calculated. Our results show that though a polycrystal is an isotropic medium in average, it is not sufficient to consider it as a metal with an effective spherical Fermi surface, since this can lead to the loss of some characteristic features of extremely anomalous skin effect in polycrystals.

DOI: 10.1103/PhysRevB.63.054202 PACS number(s): 72.90.+y, 78.66.Bz

I. INTRODUCTION

Polycrystals, being one of the states of crystalline media, are special, but very widespread case of inhomogeneous solid media, where the inhomogeneity is due to the misorientation of discrete single crystal grains. Macroscopic properties of polycrystalline solids can be described in the framework of different models of an effective isotropic medium. The problem is to calculate characteristics of such an isotropic medium when the corresponding parameters of single crystalline grains are known.

In our opinion the most accurate and physically meaningful method of calculation of effective characteristics of polycrystals goes back to the pioneering works of Lifshitz and co-workers.[1–3] In the framework of this method it is assumed that the polycrystalline medium can be described as an effective isotropic medium that is perturbed by random spatial fluctuations caused by the orientational fluctuations of the grains.

The system we consider is a single-phase polycrystalline metal. It consists of discrete grains, each of which has a regular crystalline structure. The properties of each grain are anisotropic, and crystallographic axes of the grains are randomly oriented with respect to a fixed set of laboratory axes. Then characteristics of the material measured in the laboratory coordinate system are stochastic functions of position.

In the general case an effective characteristic of a polycrystal is not a function of its value in the single crystal only, but depends on statistical properties of the medium. As a rule, spatial fluctuations can be taken into account accurately only if in the original single crystal the anisotropy of the characteristic is small and perturbation theory is applicable. The zero order term of the perturbation series is the single crystal characteristic averaged over all possible orientations of crystallites. The next order terms depend on the moments of the stochastic functions (see, for example, Ref. 4) that are the elements of the tensor single crystal characteristic measured with respect to the set of the laboratory axes. These moments can be calculated for a model polycrystal, or they are assumed to be known characteristics of the medium. There are no regular methods allowing us to calculate effective characteristics of polycrystals when anisotropy is strong.

In the case of strong anisotropy exact solutions can be found very rarely. One such example is the calculation of the effective static conductivity of a two-dimensional polycrystal, where, due to a specific symmetry transformation allowed by the equations of the problem, the exact result has been obtained for arbitrary values of two principal conductivities.[5] This result does not depend on the statistical properties of the medium (on the correlators of the conductivity in different points of the polycrystal).

The calculation of an effective characteristic of a polycrystal involves the calculation of random fields arising from the inhomogeneity of the medium (see Refs. 1–3). As a result, the calculation of effective characteristics of an unbounded polycrystal is simpler than the calculation of effective characteristics related to phenomena, where the sample surface must be taken into account. In the former case the problem is reduced to an algebraic problem, while in the latter one an integral equation must be solved (for details see Refs. 6–10). The calculation of the effective surface impedance associated with the reflection of an averaged electromagnetic wave is an example of a problem related to the sample surface. In the framework of perturbation theory the effective impedance of weakly anisotropic metal polycrystals was calculated in Refs. 8–10. Unexpectedly, it was found out that for such a complex problem an exact solution can be obtained. Recently, it was shown[11,12] that the effective impedance of strongly anisotropic polycrystalline metals can be calculated in the frequency region of the local impedance (the Leontovich) boundary conditions applicability.[13,14]

Due to very high conductivity of metals, usually the penetration depth of electromagnetic field into a metal δ is much smaller compared with the vacuum wave length $\lambda = 2\pi c/\omega$. If in the same time $\delta \ll a$, where a is a characteristic length

describing the inhomogeneity of the surface, the local impedance boundary conditions

$$\mathbf{E}_t = \hat{\zeta}[\mathbf{n}, \mathbf{H}_t], \tag{1}$$

allows us to solve an electrodynamic problem external with respect to the metal. In Eq. (1) $\mathbf{E}_t$ and $\mathbf{H}_t$ are the tangential components of electric **E** and magnetic **H** vectors at the metal surface and **n** is the unit normal vector to this surface. The two-dimensional tensor $\hat{\zeta}$ is the surface impedance tensor of the metal. In the order of magnitude $|\zeta_{\alpha\beta}| \sim \delta/\lambda \ll 1$ $(\alpha, \beta = 1,2)$. Up to the terms of the order of δ/a the tensor $\hat{\zeta}$ is an ordinary multiplying operator. If the metal surface is an inhomogeneous one, the elements of $\hat{\zeta}$ depend on the position at the surface. For a polycrystalline metal with the flat surface, a is of the order of the mean size of a grain, and the dependence of the impedance on position is defined by misorientation of the grains at the surface.

Sometimes it is sufficient to know the reflected electromagnetic field averaged over the surface inhomogeneities. By analogy with Eq. (1), we define the effective surface impedance tensor by the equation

$$\langle \mathbf{E}_t \rangle = \hat{\zeta}_{\mathrm{ef}}[\mathbf{n}, \langle \mathbf{H}_t \rangle]. \tag{2}$$

The angular brackets denote an average over the ensemble of realizations of the polycrystalline structure. If the polycrystalline medium is statistically homogeneous and untextured, in the frequency region relevant to the local impedance boundary conditions

$$\hat{\zeta}_{\mathrm{ef}} = \zeta_{\mathrm{ef}} \hat{I} = \langle \hat{\zeta}(\mathbf{x}_\parallel) \rangle, \tag{3}$$

where $\hat{I}$ is the two-dimensional unit matrix and $\mathbf{x}_\parallel$ is the two-dimensional position vector at the surface (see Refs. 11, 12). Since the only property of the medium that affects one-point averages is the rotation of the crystallographic axes of the grain with respect to the laboratory coordinate system, in Eq. (3) $\langle \cdots \rangle$ correspond to the averaging over all possible rotations of the crystallographic axes of a grain at the metal surface.

The conception of the effective surface impedance is valid if $a \ll \lambda$. Since the stochastic fields are damped out at a distance of the order of a from the metal surface, in this case beginning with a distance d, $a \ll d \ll \lambda$, the total electromagnetic field equals to its averaged value defined by $\hat{\zeta}_{\mathrm{ef}}$. In what follows we assume that

$$\delta \ll a \ll \lambda. \tag{4}$$

The result of Refs. 11,12, Eq. (3), is a nonperturbative one with respect to the dispersion of the values of the elements of the local impedance tensor. The first correction to the effective impedance due to the local impedance fluctuations[12] is $\zeta^1_{\mathrm{ef}} \sim Z^2(\delta^2/a\lambda)$, where $Z^2 = \langle [\hat{\zeta}(\mathbf{x}_\parallel) - \langle \hat{\zeta} \rangle]^2 / (\langle \zeta \rangle)^2 \rangle$. However, the local impedance boundary conditions (1) are correct only if $\delta/a \ll 1$. The terms of the order of $\delta^2/a\lambda$ are outside of the framework of the local impedance boundary conditions applicability, and the correction ζ^1_{ef} has to be omitted within the accuracy of the initial equations, Eqs. (1). Consequently, Eq. (3) allows us to calculate the effective impedance of strongly anisotropic polycrystals. Feinberg obtained a similar result while calculating the effective dielectric constant for radio waves propagating along the earth surface.[15]

Equation (3) is applicable under the conditions of both normal and anomalous skin effect. The conditions of normal skin effect correspond to the low frequency region when $l \ll \delta$ and $\omega\tau \ll 1$ (l is the electron mean free path and τ is the electron relaxation time). In Refs. 11,12 the effective impedance of various strongly anisotropic polycrystalline media has been calculated under the conditions of normal skin effect. In sufficiently clean metals, skin effect clearly shows an anomalous character when the temperature is low and the electron mean free path l exceeds the penetration depth δ. At the same time, the frequency ω can be much less than $1/\tau$.

In the present publication we concentrate on the analysis of the effective surface impedance of polycrystalline metals under the conditions of extremely anomalous skin effect ($l \gg \delta$, $\omega\tau \ll 1$). In this case the relation between the current **j** and the electric field strength **E** is nonlocal and Maxwell's equations turn into the system of integrodifferential equations. We would like to point out that in the papers of Lifshitz *et al.*,[1–3] as well as in the following studies (as an example we cite Refs. 16–18), calculations of effective characteristics of polycrystals were based on the solution of differential equations with stochastic coefficients. The study of anomalous skin effect in polycrystals appears to be the first example of an analysis of stochastic integrodifferential equations.

The characteristic features of the surface impedance of single crystal metals under the conditions of extremely anomalous skin effect can be found in a lot of textbooks of electron theory of metals (see, for example, Ref. 19). Here we only mention the ones we need in our analysis of the effective impedance of polycrystals.

First, the impedance of single crystals is sensitive to orientation of the surface with respect to the crystallographic axes. Secondly, under the conditions of anomalous skin effect the impedance depends on the geometry of the Fermi surface of the metal. The Fermi surfaces of real metals are extremely complex and differ significantly for different metals.[19,20] In certain metals they are closed surfaces (sets of individual identical surfaces, each of which is situated in its respective Brillouin zone), in other metals the Fermi surfaces are open, passing through the whole momentum space. Thirdly, the inequality $l \gg \delta$, or $kl \gg 1$ ($k = |\mathbf{k}|$, $\mathbf{k}$ is the electromagnetic field wave vector), selects electrons from ''the belt'' $\mathbf{k}\mathbf{v}_F = 0$ at the Fermi surface, $\mathbf{v}_F$ is the velocity of an electron on the Fermi surface. Other electrons are ineffective[19] and do not take part in the reflection of electromagnetic waves. As a result, the leading term of the impedance does not depend on the electron mean free path l.

When calculating the impedance of a polycrystal, an averaging over the orientation of the crystallographic axes of the grain at the metal surface with respect to the direction of the normal to the surface has to be done (see below). When the direction of the normal to the metal surface changes,

''the belt'' moves along the Fermi surface. Thus, the impedance of the polycrystal is defined by all electrons from the Fermi surface even under the conditions of extremely anomalous skin effect. The averaging leads to an isotropization. It is usual to think of an isotropic metal as of a metal with a spherical Fermi surface. The question is, if this evidently model assumption is correct for the description of anomalous skin effect in polycrystals.

Our results show that being a characteristic of a medium which is isotropic on the average, the effective impedance of a polycrystal composed of single crystal grains with complex Fermi surface depends on the details of the geometry of the Fermi surface. According to Refs. 11,12 the calculation of the effective impedance of polycrystals involves two steps. The first step is the calculation of the impedance of the crystal metal for an arbitrary orientation of the crystallographic axes with respect to the metal surface. The second step is the averaging over all possible orientations of the crystallographic axes. The first step requires the definition of electrons providing the maximal contribution to the conductivity when $kl \gg 1$. It is well known, the more the conductivity, the less the impedance. The second step (the averaging) selects the calculated impedances choosing the maximal. Thus, the effective impedance is the result of solution of a nontrivial minimax problem.

The outline of this paper is as follows. In Sec. II under the conditions of anomalous skin effect the general expression for the effective impedance of a polycrystalline metal composed of single crystal grains with an arbitrary Fermi surface is obtained. In Sec. III we calculate the effective impedance for different model Fermi surfaces. In Sec. IV we analyze the effect of the change of the topology of the Fermi surface on the value of the effective impedance of polycrystals.

II. EFFECTIVE IMPEDANCE OF POLYCRYSTAL UNDER CONDITIONS OF ANOMALOUS SKIN EFFECT

A. The local surface impedance calculation

To make use of Eq. (3), we need to know the explicit form of the local impedance $\hat{\zeta}(\mathbf{x}_\parallel)$. Let us assume that the grains are sufficiently large:

$$a \gg l. \tag{5}$$

In this case the current density $\mathbf{j}$ in a grain is nearly the same as in the single crystal rotated with respect to the laboratory axes in the same way as the given particular grain. Consequently, $\hat{\zeta}(\mathbf{x}_\parallel)$ approximately equals to the impedance of the single crystal whose crystallographic axes are rotated with respect to the laboratory axes in the same way as the ones of the grain at the point $\mathbf{x}_\parallel$.

It is known[21] that when the relaxation time approximation (the τ approximation) is used and the specular reflection of conductive electrons from the metal surface is assumed, the problem of the surface impedance calculation, detecting the main features of the anomalous skin effect, is simplified significantly. (For the detailed discussion see Ref. 10.) In this case the elements of the surface impedance tensor of a single crystal metal are

$$\zeta_{\alpha\beta} = \frac{1}{\pi}\int_0^\infty \zeta_{\alpha\beta}(k)\,dk, \tag{6a}$$

where the Fourier coefficients $\zeta_{\alpha\beta}(k)$ are expressed in terms of the elements of the reciprocal tensor $\zeta^{-1}_{\alpha\beta}(k)$,

$$\zeta^{-1}_{\alpha\beta}(k) = -\frac{c}{2i\omega}\left[k^2\delta_{\alpha\beta} - \frac{4\pi i\omega}{c^2}\sigma_{\alpha\beta}(k)\right]. \tag{6b}$$

The two-dimensional tensor $\zeta_{\alpha\beta}$ $(\alpha,\beta = 1,2)$ is defined with respect to the laboratory coordinate system. The axes 1 and 2 of this coordinate system are placed on the metal surface and the axis 3 is directed along the normal $\mathbf{n}$ to the surface.

In Eqs. (6a),(6b) $\sigma_{ik}(k)$ are the Fourier coefficients of the elements of the conductivity tensor calculated for the unbounded single crystal metal. In the τ approximation[19,21]

$$\sigma_{ik}(\mathbf{k}) = \frac{2e^2\tau}{(2\pi\hbar)^3}\int \frac{v_i v_k}{v[1 + i\mathbf{k}\mathbf{v}\tau]}\,dS, \tag{7}$$

where the integration is carried out over the Fermi surface in one Brillouin zone. The Fermi surface is defined by an equation $\varepsilon(\mathbf{p}) = \varepsilon_F$; ε_F is the Fermi energy; $\mathbf{v}(\mathbf{p}) = \partial\varepsilon(\mathbf{p})/\partial\mathbf{p}$ is the velocity of an electron at the Fermi surface and $v = |\mathbf{v}(\mathbf{p})|$. When calculating the surface impedance the wave vector $\mathbf{k}$ is supposed to be directed along the normal to the metal surface.

It is of interest that in the limit $kl \gg 1$ $(l \sim v\tau)$ in spite of such complicated dependence of $\sigma_{ik}(\mathbf{k})$ on the Fermi surface geometry, the conductivity tensor averaged over all orientations of the crystallographic axes is given by the very simple expression[10]

$$\langle \sigma_{ik}(\mathbf{k})\rangle = \sigma_a(k)(\delta_{ik} - k_i k_k/k^2), \quad \sigma_a(k) = \frac{\pi e^2 S_F}{2(2\pi\hbar)^3 k}, \tag{8}$$

where S_F is the total area of the Fermi surface. Equations (8) define the Fourier coefficients of the elements of the conductivity tensor of an isotropic conductor with a spherical Fermi surface. The impedance of such a conductor is $\zeta_{\alpha\beta} = \zeta_a\delta_{\alpha\beta}$, where

$$\zeta_a = \frac{2(1 - i\sqrt{3})}{3\sqrt{3}}\left(\frac{\omega\delta_a}{c}\right), \quad \delta_a = \left(\frac{4\pi c^2\hbar^3}{\omega e^2 S_F}\right)^{1/3}; \tag{9}$$

δ_a is the relevant electric field penetration depth.[21]

For slightly anisotropic polycrystals Eqs. (9) define the effective impedance in the zeroth approximation with respect to anisotropy. Apparently, the small anisotropy means either that the Fermi surface is regularly close to a sphere (for example, it is an ellipsoid with nearly equal principal axes), or the ''weight'' of the regions where the Fermi surface deviates from the sphere is small. With regard to the effective impedance calculation the Fermi surface anisotropy can be considered small, if

$$\Delta^2 = \left|\frac{4}{\pi S_F^2}\int\int \frac{dS_1\,dS_2(\vec{\nu}_1\vec{\nu}_2)^2}{\sqrt{1 - (\vec{\nu}_1\vec{\nu}_2)^2}} - 1\right| \ll 1. \tag{10}$$

In Eq. (10) the double integration is carried out over the Fermi surface; $\vec{\nu}=\mathbf{v}(\mathbf{p})/v(\mathbf{p})$. Equation (9) gives the leading term of the expression for the effective impedance. The first correction to ζ_a is proportional to Δ^2 (see Ref. 12). When anisotropy is strong, Eqs. (9) are inapplicable. In what follows, we use σ_a, ζ_a, and δ_a only as characteristic values of the conductivity, the impedance and the penetration depth relating to the given Fermi surface.

In view of the following averaging of the local surface impedance tensor (6), we rewrite Eq. (7) for the conductivity $\sigma_{ik}(\mathbf{k})$ in the form

$$\sigma_{ik}(\mathbf{k})=\sigma_a(k)S_{ik}(\mathbf{k}); \tag{11a}$$

where σ_a is given by Eq. (8) and $S_{ik}(\mathbf{k})$ is a dimensionless tensor. As a rule, when $kl\gg 1$, leading terms in the expressions for the elements of this tensor depend on the Fermi surface geometry and the orientation of the crystallographic axes only:

$$S_{ik}(\mathbf{k}/k)=\frac{4}{S_F}\int \nu_i\nu_k\delta(\mathbf{kv}/kv)dS, \quad \nu_i=\frac{v_i}{v} \tag{11b}$$

and $\mathbf{k}=(0,0,k)$. It is clearly seen that only electrons from ''the belt'' $\mathbf{kv}=0$ contribute to the elements of the tensor S_{ik}. Usually the elements $S_{\alpha\beta}(\mathbf{k}/k)$ $(\alpha,\beta=1,2)$ of the tensor $S_{ik}(\mathbf{k}/k)$ are of the order of unity and, consequently, the transverse conductivities $\sigma_{\alpha\beta}$ are of the order of σ_a. In the same approximation the elements $S_{i3}(\mathbf{k}/k)=0; i=1,2,3$. When in Eqs. (7) next terms in the small parameter $1/kl$ are taken into account, $\sigma_{i3}(\mathbf{k})\sim\sigma_a/kl$. If by any reason the tangential elements $S_{\alpha\beta}$ of the tensor (11b) are equal to zero, all the elements of the tensor $\sigma_{ik}(k)\sim\sigma_a/kl$. In Sec. III we examine several examples of such extraordinary situations, but here we restrict ourselves to Eqs. (11b).

Usually it is most covenient to calculate the elements of the tensor $\hat{S}$ with respect to the crystallographic axes. Let γ denote the rotation of the crystallographic axes with respect to the laboratory axes through the three Euler angles $\theta_k,\psi_k,\varphi_k$. There are some different ways of the Euler angles definition.[22] In our calculations we supposed that the set of crystallographic unit vectors $\mathbf{e}_i^{(\mathrm{cr})}$ was obtained from the fixed set of the laboratory unit vectors $\mathbf{e}_i$ by three sequential rotations: (1) the rotation about the angle φ_k about the axis 3; (2) the rotation of the obtained set of the unit vectors about the angle θ_k about the new axis 2; (3) the rotation of the obtained set of the unit vectors about the angle ψ_k about the new axis 3. The rotation matrix was defined as $\alpha_{ik}=(\mathbf{e}_i\mathbf{e}_k^{(\mathrm{cr})})$.

Let $k_i^{(\mathrm{cr})}$ be the components of the wave vector and $S_{ik}^{(\mathrm{cr})}(\mathbf{k})$ be the elements of the tensor $\hat{S}$ with respect to the set of crystallographic axes. Then $k_i^{(\mathrm{cr})}(\gamma)=k\alpha_{3i}$, and, according to Eq. (11b), the elements $S_{ik}^{(\mathrm{cr})}(\mathbf{k})$ are functions of the Euler angles. Finally, the elements of the conductivity tensor with respect to the laboratory axes are

$$\sigma_{ik}(k;\gamma)=\sigma_a(k)S_{ik}(\gamma); \quad S_{ik}(\gamma)=\alpha_{ip}(\gamma)\alpha_{kq}(\gamma)S_{pq}^{(\mathrm{cr})}(\gamma). \tag{12}$$

Now we can write down the Fourier coefficients $\zeta_{\alpha\beta}(k)$ in terms of the elements of the dimensionless tensor $\hat{S}(\gamma)$:

$$\zeta_{\alpha\beta}(x;\gamma)=-i\frac{2\omega\delta_a}{c}\delta_a x[x^3\delta_{\alpha\beta}-iZ_{\alpha\beta}(\gamma)]/z(x;\gamma); \tag{13a}$$

$$Z_{11}(\gamma)=S_{22}(\gamma); \quad Z_{12}(\gamma)=S_{12}(\gamma); \quad Z_{22}(\gamma)=S_{11}(\gamma). \tag{13b}$$

Here $x=k\delta_a$ [δ_a is defined by Eq. (9)] and the function $z(x;\gamma)$ is

$$z(x;\gamma)=[x^3-iS_1(\gamma)][x^3-iS_2(\gamma)], \tag{13c}$$

where $S_1(\gamma)$ and $S_2(\gamma)$ are the principal values of the two-dimensional tensor $S_{\alpha\beta}(\gamma)$:

$$S_{1,2}(\gamma)=\frac{1}{2}[S_{11}(\gamma)+S_{22}(\gamma)\pm R(\gamma)],$$

$$R(\gamma)=\sqrt{[S_{11}(\gamma)-S_{22}(\gamma)]^2+4S_{12}^2(\gamma)}. \tag{13d}$$

Equation (13c) defines the poles of the integrand in the expressions (6a) for the elements of the impedance tensor $\zeta_{\alpha\beta}(\gamma)$. After the integration is carried out (the method of integration can be found, for example, in Ref. 21), we obtain the elements of the impedance tensor as functions of γ:

$$\zeta_{11}(\gamma)=\frac{1}{2}\zeta_a\{[S_1{}^{-1/3}(\gamma)+S_2{}^{-1/3}(\gamma)] + s(\gamma)[S_1{}^{-1/3}(\gamma)-S_2{}^{-1/3}(\gamma)]\}, \tag{14a}$$

$$\zeta_{22}(\gamma)=\frac{1}{2}\zeta_a\{[S_1{}^{-1/3}(\gamma)+S_2{}^{-1/3}(\gamma)] - s(\gamma)[S_1{}^{-1/3}(\gamma)-S_2{}^{-1/3}(\gamma)]\}, \tag{14b}$$

with ζ_a from Eq. (9) and

$$s(\gamma)=\frac{[S_{11}(\gamma)-S_{22}(\gamma)]}{R(\gamma)}. \tag{14c}$$

In Eqs. (13),(14) the dependence of all the terms on the Euler angles (on the set γ) is shown explicitly. We do not write down the expression for ζ_{12}, since that element of the local impedance tensor does not contribute to ζ_{ef}.

B. The effective surface impedance calculation

In accordance with Eq. (3) the elements of the tensor $\hat{\zeta}_{\mathrm{ef}}$ are the averages over the rotations γ of the local impedance tensor (14). With regard to our definition of the Euler angles the direct calculation showed that the Euler angle φ_k entered only the expression for the function $s(\gamma)$. The structure of this function was: $s(\gamma)=S(\theta_k,\psi_k)\sin 2\varphi_k + C(\theta_k,\psi_k)\cos 2\varphi_k$. We also showed that the nondiagonal element S_{12} of the tensor $\hat{S}(\gamma)$ depended on the angle φ_k in the same way as the function $s(\gamma)$. Then, after the averaging over the angle φ_k, it is evident that

$$\zeta_{\rm ef}=\frac{1}{2}\zeta_a\langle S_1^{-1/3}(\theta_k,\psi_k)+S_2^{-1/3}(\theta_k,\psi_k)\rangle,$$

$$\langle\cdots\rangle=\frac{1}{4\pi}\int_0^{\pi}\sin\theta_k\,d\theta_k\int_0^{2\pi}\cdots d\psi_k. \qquad (15)$$

With the aid of Eq. (15), the effective surface impedance of a polycrystalline metal can be calculated (at least numerically), if the equation of the Fermi surface of the original single crystal is known.

Equation (15) is rather formal. Below we present the formulas obtained from Eq. (15) for a Fermi surface which is a surface of revolution. The derivation of Eqs. (16) is presented in Appendix A.

Let the rotation axis of the Fermi surface coincide with the crystallographic axis *z*. (For axially symmetric Fermi surfaces we use a subscript $\perp$ for the vectors in the plane perpendicular to the axis *z*. The subscripts *z* and $\perp$ are used only for the vectors written with respect to crystallographic axes.) Let the equation of the Fermi surface written with respect to the crystallographic axes be $\varepsilon_F=\varepsilon(p_\perp,p_z)$, $p_\perp=|\mathbf{p}_\perp|$. For such a surface the functions $S_{1,2}$ depend on the spherical Euler angle θ_k only:

$$S_1=\frac{16}{S_F\sin\theta_k\tan\theta_k}\int p_\perp\Phi(p_\perp,\tan\theta_k)dp_\perp;$$

$$S_2=\frac{16\tan\theta_k}{S_F\sin^3\theta_k}\int p_\perp\frac{dp_\perp}{\Phi(p_\perp,\tan\theta_k)}, \qquad (16a)$$

where

$$\Phi(p_\perp,\tan\theta_k)=\sqrt{\frac{v_\perp^2\tan^2\theta_k-v_z^2}{v_z^2}}. \qquad (16b)$$

Consequently, the averaging is reduced to the integration over the Euler angle θ_k:

$$\langle S_\alpha{}^{-1/3}\rangle=\int_0^{\pi/2}\sin\theta_k S_\alpha{}^{-1/3}\,d\theta_k;\quad \alpha=1,2. \qquad (17)$$

We introduced the transverse speed of an electron on the Fermi surface $v_\perp=\partial\varepsilon(p_\perp,p_z)/\partial p_\perp$ and the projection of an electron velocity on the axis *z*: $v_z=\partial\varepsilon(p_\perp,p_z)/\partial p_z$. In Eqs. (16a) the integration is carried out over the part of the Fermi surface, where $v_z>0$ and the radicand of the function $\Phi(p_\perp,\tan\theta_k)$ is positive. If the Fermi surface is a multiply connected surface, the integration is spread over all of its parts.

Equations (16) and (17) are rather simple. They allow to analyze the influence of the Fermi surface geometry on the value of the effective surface impedance.

In conclusion of this section we would like to note that Eq. (15) [as well as Eqs. (16) and (17)] for the effective impedance are based on the approximation (11b) for the elements of the conductivity tensor $\sigma_{ik}(\mathbf{k})$, which is supposed to be true for an arbitrary orientation of the wave vector $\mathbf{k}$ with respect to the crystallographic axes. In this case the difference between $\zeta_{\rm ef}$ and ζ_a is in a real numerical factor $\frac{1}{2}\langle S_1{}^{-1/3}+S_2{}^{-1/3}\rangle$. Then, comparing Eqs. (15) and (9), we see that effectively the polycrystal is an isotropic conductor with the spherical Fermi surface, whose area is equal $S_F^{(a)}$,

$$S_F^{(a)}=S_F\left[\frac{1}{2}\langle S_1^{-1/3}+S_2^{-1/3}\rangle\right]^{-3}, \qquad (18)$$

S_F is the true area of the Fermi surface. Of course, in this case the effective impedance reproduces all the main characteristic features of the impedance of an isotropic metal. Namely, $\zeta_{\rm ef}$ does not depend on the mean free path *l*, and the relation between the real and the imaginary parts of $\zeta_{\rm ef}$ is given by the factor $(1-i\sqrt{3})$ which enters the expression (9) for ζ_a. Several examples of the Fermi surfaces for which these general rules are not true are presented below in Secs. III B and III C.

III. EFFECTIVE SURFACE IMPEDANCE OF POLYCRYSTALS COMPOSED OF THE GRAINS WITH SOME MODEL FERMI SURFACES

In this section, we present some examples of the effective impedance calculation for different model polycrystals. We assume that Fermi surfaces of original single crystals have rather simple forms. Although the examples discussed below cannot be directly related to real metals, they allow us to solve the problem accurately (up to numerical factors) and to show clearly the dependence of the effective impedance on the geometry of the Fermi surface.

A. Ellipsoidal Fermi surface

Let the Fermi surface be an uniaxial ellipsoid. Such a surface is the simplest example of a closed nonspherical Fermi surface. With respect to the crystallographic axes, the equation of the Fermi surface is

$$\varepsilon_F=\frac{1}{2m_\perp}p_\perp^2+\frac{1}{2m_z}p_z^2. \qquad (19)$$

Let us set

$$p_*=(2m_\perp\varepsilon_F)^{1/2},\quad \mu=m_z/m_\perp. \qquad (20)$$

If $\mu\ll1$, the Fermi surface is close to a disk; if $\mu\gg1$, it is a needle-shaped one. In terms of p_* and μ the area S_F of the surface (19) is $S_F=4\pi p_*^2Q(\mu)$,

$$Q(\mu<1)=\frac{1}{2}\left\{1+\frac{\mu}{2\sqrt{1-\mu}}\ln\left[\frac{1+\sqrt{1-\mu}}{1-\sqrt{1-\mu}}\right]\right\},$$

$$Q(\mu>1)=\frac{1}{2}\left\{1+\frac{\mu}{\sqrt{\mu-1}}\arcsin\sqrt{\frac{\mu-1}{\mu}}\right\}. \qquad (21)$$

We calculated the functions $S_{1,2}(\theta_k)$ according to Eqs. (16):

$$S_1(\theta_k;\mu)=\frac{\mu}{Q(\mu)\sqrt{\cos^2\theta_k+\mu\sin^2\theta_k}},$$

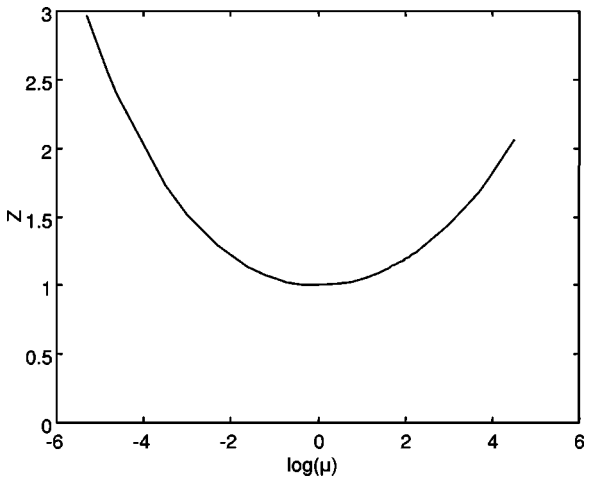

FIG. 1. The function $Z=Z(\mu)$ defined by Eq. (23b).

$$S_2(\theta_k;\mu)=\frac{\mu}{Q(\mu)[\cos^2\theta_k+\mu\sin^2\theta_k]^{3/2}}. \tag{22}$$

If the ellipsoid is strongly flattened or strongly elongated, at least one of the principle values of the tensor $S_{\alpha\beta}$ (they are S_1 and S_2) is singularly small: $S_{1(2)}\sim\mu$ if $\mu\ll 1$, and $S_2\sim 1/\mu$ if $\mu\gg 1$. In other words, at least one of the principle conductivities is singularly small compared with the averaged conductivity σ_a.

With regard to Eq. (17), our result for the effective impedance in the case of the ellipsoidal Fermi surface (19) is

$$\zeta_{\rm ef}^{(el)}=\zeta_a Z(\mu), \tag{23a}$$

where ζ_a is defined by Eq. (9) and

$$Z(\mu)=\frac{1}{2}\left(\frac{Q(\mu)}{\mu}\right)^{1/3}\int_0^1 dx\, M^{1/6}(x;\mu)[1+M^{1/3}(x;\mu)];$$

$$M(x;\mu)=x^2+\mu(1-x^2). \tag{23b}$$

The function $Z(\mu)$ is presented in Fig. 1. When the ellipsoid is strongly flattened or strongly elongated, $Z(\mu)\gg 1$:

$$Z(\mu)\approx\frac{5}{8}\left(\frac{1}{2\mu}\right)^{1/3}\quad \text{if}\quad \mu\ll 1\quad \text{and}$$

$$Z(\mu)\approx\frac{\pi}{8}\left(\frac{\pi\mu}{4}\right)^{1/3}\quad \text{if}\quad \mu\gg 1. \tag{23c}$$

Consequently, in these cases the effective impedance $\zeta_{\rm ef}^{(el)}\gg\zeta_a$. Finally, according to Eq. (18) the effective area of the Fermi surface (19) relating to the effective impedance calculation is $S_F^{(a)}=S_F Z^{-3}(\mu)$.

Thus, although usually ζ_a can be used as an estimate of the effective impedance of a polycrystal, there are situations when $\zeta_{\rm ef}$ differs from ζ_a significantly. In our example that are the cases of strongly flattened and strongly elongated ellipsoidal Fermi surfaces (19). At such surfaces for an arbitrary directed vector **k** ''the belts'' $\mathbf{kv}=0$ are very small. They are placed mainly near the vertexes of the ellipsoid. This is the reason why in these cases at least one of the principle conductivities is much less than σ_a and, consequently, the effective impedance is much greater than ζ_a.

An elongated ellipsoid resembles a cylinder. The case of an open cylindrical Fermi surface is discussed in the next subsection.

B. Open cylindrical Fermi surface

The simplest model of an open Fermi surface is an infinitely long cylindrical tube. Let the axis z of the crystallographic coordinate system be the cylindrical axis. The equation of such a surface in a certain Brillouin zone is

$$\varepsilon_F=\frac{p_\perp^2}{2m};\quad -p_m<p_z<p_m, \tag{24}$$

where $2p_m$ is the length of Brillouin zone along the direction z. (In terms of the electron number density n we have $p_m=n\pi^2\hbar^3/m\varepsilon_F$.)

For the cylindrical Fermi surface (24), an electron velocity **v** is in the plane perpendicular to the axis z. Since $v_z=0$, when calculating the effective impedance we cannot use Eqs. (16) directly. We have to repeat the calculation beginning from the derivation of the proper expressions for the elements of the tensor $\hat{S}$.

First of all let us show that in this case to calculate the impedance, it is not sufficient to know the elements of the tensor $\hat{S}$ only up to the leading terms (11b) of the series expansion in powers of the small parameter $1/kl$. Indeed, if we make use of Eqs. (11b) and calculate the elements of the tensor $\hat{S}$ with respect to the crystallographic coordinate system and then pass to the laboratory coordinate system with the aid of Eq. (12), it easy to see that

$$S_{11}(\gamma)=\frac{4}{\pi\sin\theta_k}\sin^2\varphi_k,\quad S_{12}(\gamma)=-\frac{2}{\pi\sin\theta_k}\sin 2\varphi_k,$$

$$S_{22}(\gamma)=\frac{4}{\pi\sin\theta_k}\cos^2\varphi_k, \tag{25}$$

and, of course, $S_{13}=S_{23}=S_{33}=0$. With regard to Eqs. (13d) this means that one of the principal values of the tensor $S_{\alpha\beta}$, namely, S_2, is equal zero. Next, if $S_2=0$, the denominator in the expressions (13a) for the Fourier coefficients of the elements of the impedance tensor is $z(x=k\delta_a;\gamma)=x^3[x^3-iS_1(\gamma)]$, and the integrals (6a) defining the impedance $\zeta_{\alpha\beta}$ diverge. To get rid of the divergence, we have to calculate the next terms of the tangential conductivities.

We use Eq. (7) and by analogy with Eq. (11a) we write the elements of the conductivity tensor in the form

$$\sigma_{ik}=\sigma_a(k)S_{ik}(\gamma;1/kl), \tag{26}$$

with σ_a defined by Eq. (8), where $S_F=4\pi p_m\sqrt{2m\varepsilon_F}$ is the lateral area of the cylinder. The simple form of the Fermi surface allowed us to calculate the elements of the tensor $S_{ik}(\gamma;1/kl)$ for an arbitrary value of $1/kl$. With this result in hand we calculated the principle values $S_1(\gamma;1/kl)$ and $S_2(\gamma;1/kl)$ up to the terms of the order of $1/kl$:

$$S_1(\gamma;1/kl)\approx\frac{4}{\pi\sin\theta_k}\left[1-\frac{1}{kl\sin\theta_k}\right];$$

$$S_2(\gamma;1/kl)\approx\frac{4}{\pi kl}\cot^2\theta_k. \tag{27}$$

The anomalously small conductivity $\sigma_2=\sigma_a S_2$ contributes to the leading terms in the expressions (6a) for the elements the impedance tensor $\zeta_{\alpha\beta}(\gamma)$. It defines unusual behavior of the surface impedance of a metal with the cylindrical Fermi surface. First, simple direct calculations showed: the additional small factor $1/kl$ in the expression for S_2 results in the additional big factor $(l/\delta_a)^{1/4}$ in the expressions for the elements of the surface impedance tensor; δ_a is defined by Eq. (9). [It can be easily seen after the substitution of the dimensionless variable $x=k\delta_a$ in the expressions for the Fourier coefficients $\zeta_{\alpha\beta}(k;\gamma)$.] Next, the poles of the integrand of Eq. (6a) are the zeros of the function $z(x;\gamma)$ defined by Eq. (13c). However, now the poles related to $S_2(\gamma;1/kl)$ are not the roots of the third-degree equation but of the fourth-degree equation $x^4-4i\cot^2\theta_k/\pi=0$. We showed that as a result, for the single crystal with the cylindrical Fermi surface the relation between the real and the imaginary parts of the surface impedance was defined not by the usual factor $(1-i\sqrt{3})$, but by the factor $e^{-3i\pi/8}$.

The aforementioned specific features are inherent in polycrystals composed of the single crystal grains with the cylindrical Fermi surface. After calculating the elements of the single crystal impedance tensor $\zeta_{\alpha\beta}(\gamma)$ and consequent averaging with respect to all possible rotations γ, we obtained

$$\zeta_{\rm ef}^{(cyl)}=\frac{1}{8}\left(\frac{\omega\delta_a}{c}\right)\left(\frac{l}{4\pi\delta_a}\right)^{1/4}e^{-3i\pi/8}\Gamma^2(1/4), \tag{28}$$

where $\Gamma(x)$ is the gamma function. We see that the absolute value of $\zeta_{\rm ef}^{(cyl)}$ is much greater than the typical value $|\zeta_a|$: $|\zeta_{\rm ef}^{(cyl)}|\sim|\zeta_a|(l/\delta_a)^{1/4}$ [compare Eqs. (28) and (9)].

C. Cubic Fermi surface

Let the Fermi surface be a cube. Let the origin of the set of the crystallographic axes be at the center of the cube. With respect to crystallographic axes the sides of the cube are the planes

$$p_i^{(\rm cr)}=\pm p_F\quad(i=1,2,3); \tag{29}$$

the edges of the cube are the intersections of the planes (29). At the sides of the cube the velocity $v_i^{(\rm cr)}=\pm v_F$ (on the opposite sides the directions of the vector **v** are opposite); the Fermi energy is $\varepsilon_F=\mathbf{vp}$.

The surface (29) is not the surface of revolution and, consequently, Eqs. (16) are not applicable. Moreover, it is evident that for an arbitrary direction of the wave vector **k** there are no ''belts'' on the cubic Fermi surface where $\mathbf{kv}=0$. This means that the approximation (11) for $\sigma_{ik}(k;\gamma)$, as well as the general equations (15), are not applicable either. So, in this case, the starting point of our calculation was the general expression (7) for the Fourier coefficients $\sigma_{ik}(\mathbf{k})$.

When the Fermi surface is a cube for an arbitrary value of the parameter $kl=kv_F\tau$, it is very easy to perform the integration in Eq. (7) with respect to crystallographic coordinate system. It is evident that the only nonzero elements of the tensor $\sigma_{ik}^{(\rm cr)}$ are its diagonal elements. With respect to the set of laboratory axes the elements of the tensor $\sigma_{ik}(k;\gamma)$ are

$$\sigma_{ik}(k;\gamma)=\sigma_a S_{ik}(kl;\gamma),$$

$$S_{ik}(kl;\gamma)=\frac{4kl}{3\pi}\sum_{q=1}^{3}\frac{\alpha_{iq}\alpha_{kq}}{[1+(kl)^2\alpha_{3q}^2]}; \tag{30}$$

σ_a is given by Eq. (8) with S_F being the lateral area of the cube: $S_F=24p_F^2$.

When $kl\gg1$ from Eqs. (30) it follows that for almost all the Euler angles the series expansion of all the elements of the tensor S_{ik} begins with the terms of the order of $1/kl$. Thus, when $kl\gg1$, for the cubic Fermi surface all the elements of the conductivity tensor have the additional factor $1/kl$ and are much less than the characteristic conductivity σ_a. It worth to be mentioned, that nevertheless the elements of the averaged conductivity $\langle\sigma_{ik}(k;\gamma)\rangle$ as before are given by Eqs. (8). The point is that if we neglect 1 in the denominator of the expression for S_{ik}, the averaging of Eqs. (30) lead to divergent integrals.

However, no divergence of the integrals (6a) occurred when $S_{ik}\approx F_{ik}/kl$ $(F_{ik}=\Sigma_{q=1}^{3}\alpha_{iq}\alpha_{kq}/\alpha_{3q}^2)$ were used to calculate the Fourier coefficients $\zeta_{\alpha\beta}(k;\gamma)$. We showed that in the same way as in the case of the cylindrical Fermi surface, due to the additional small factor $1/kl$ the poles of $\zeta_{\alpha\beta}(k;\gamma)$ were the roots of fourth degree equations.

When the calculated Fourier coefficients $\zeta_{\alpha\beta}(k;\gamma)$ were substituted in Eq. (6a) and the integration was carried out, we obtained the elements of the impedance tensor $\zeta_{\alpha\beta}^{(\rm cube)}(\gamma)$ of a single crystal with the cubic Fermi surface. They depended on all of the three Euler angles and showed the same specific features as in the case of the cylindrical Fermi surfaces. Namely, they had the additional big factor $(l/\delta_a)^{1/4}$, and the relations between their real and imaginary parts were defined by the unusual factor $e^{-3i\pi/8}$.

These specific features survive in polycrystals. After the averaging of $\zeta_{\alpha\beta}^{(\rm cube)}(\gamma)$ with respect to all possible rotations γ we obtained the effective impedance in the case of the cubic Fermi surface:

$$\zeta_{\rm ef}^{(\rm cube)}=\frac{N}{4}\left(\frac{\omega\delta_a}{c}\right)\left(\frac{3\pi l}{\delta_a}\right)^{1/4}e^{-3i\pi/8};\quad N=\langle F_1^{-1/4}+F_2^{-1/4}\rangle, \tag{31}$$

where $F_{1(2)}$ were the principle values of the two-dimensional tensor $F_{\alpha\beta}$. Numerical evaluation of the factor N gave $N=0.892$.

Of course, there are no cubic Fermi surfaces in real life. But there are metals whose Fermi surfaces are close to polyhedrons (see, for example, Ref. 23). In this connection, let us estimate when smoothing of the edges and the vertexes of the cube does not lead to a substantial change of the result (31). Since the value of the local surface impedance (and, consequently, the value of the effective impedance) is de-

fined by the elements of the conductivity tensor $\sigma_{ik}(\mathbf{k})$, it is sufficient to estimate when the contribution to $\sigma_{ik}(\mathbf{k})$ from the smoothing regions is much less than the contribution from the sides of the cube. According to Eqs. (30) and (8), when $kl \gg 1$ the contribution to the conductivity from the sides of the cube is of the order of $\sigma^{(\mathrm{cube})} \sim e^2 p_F^2 / k(kl)\hbar^3$.

Suppose δp_v is the characteristic size of the smoothing region near the vertexes of the cube. With regard to Eqs. (11) the contribution to the conductivity from the regions near the vertexes is of the order of $\delta\sigma^{(v)} \sim e^2 (\delta p_v)^2 / k\hbar^3$. Next, the characteristic size of the smoothing region in the direction along an edge of the cube is of the order of p_F. Suppose δp_{ed} is the characteristic size of the smoothing region in the directions perpendicular to the edge. Then the contribution to the conductivity from the regions near the edges is of the order of $\delta\sigma^{(\mathrm{ed})} \sim e^2 p_F \delta p_{\mathrm{ed}} / k\hbar^3$. If $\delta p_{\mathrm{ed}} \sim \delta p_v \sim \delta p$, the value of δp is limited by the inequality $\delta\sigma^{(\mathrm{ed})} \ll \sigma^{(\mathrm{cube})}$:

$$\delta\sigma^{(v)}, \delta\sigma^{(\mathrm{ed})} \ll \sigma^{(\mathrm{cube})}, \quad \text{if} \quad \delta p \ll \frac{p_F}{kl}. \tag{32}$$

With respect to polycrystals with nearly cubic Fermi surfaces, Eq. (32) defines the limits of the result (31) applicability.

Usually under the conditions of extremely anomalous skin effect, the impedance does not depend on the mean free path l (see, for example, Ref. 19). This general conclusion is inapplicable for some specific Fermi surfaces. Our results show that it fails for an open cylindrical and for a cubic Fermi surface (or more generally, when the Fermi surface is a polyhedron). This conclusion is true both for single crystals and polycrystals. In these cases the effective impedance depends on the mean-free path l and significantly exceeds the characteristic value $|\zeta_a|$: $|\zeta_{\mathrm{ef}}| \sim (l/\delta_a)^{1/4} |\zeta_a|$. In addition the relation between the real and the imaginary parts of the effective impedance is defined by unusual factor $\exp(-3i\pi/8)$.

Equations (28) and (31) were obtained as a result of direct calculations and formally no further explanations are needed. However, the calculations are rather tedious, and the answer is not obvious. To visualize the result we use the Pippard method.[24] Pippard called it the method of ineffective electrons.

Following Pippard, under the conditions of extremely anomalous skin effect the impedance can be calculated in the same way as in the case of normal skin effect, if we take into account that only a small part of conduction electrons proportional to δ/l (electrons from ''the belt'' at the Fermi surface) takes part in the reflection of electromagnetic waves. Pippard used the standard formulas for the penetration depth and the surface impedance, where the conductivity $\sigma_n \sim ne^2 l / p_F$ was replaced by the effective value $\sigma_P \sim \sigma_n (\delta/l)$.

In other words, due to ''the belts,'' we cannot simply omit 1 in the denominator of expression (7) for the conductivity $\sigma_{ik}(\mathbf{k})$. Now let us suppose that in the limit $kl \gg 1$ when calculating the principal values of the transverse conductivity $\sigma_{\alpha\beta}(\mathbf{k})$ for a given direction of the wave vector $\mathbf{k}$, we can neglect 1 without the divergence of the integrals over the Fermi surface at least for one of the principal values. Then this principal value is $kl \sim l/\delta$ times less than the regular value of the conductivity. Since the impedance is defined by the smaller of the principal conductivities, the additional small factor δ/l appears in the effective conductivity. Then $\sigma_P \sim \sigma_n (\delta/l)^2$. Consequently,

$$\delta_P \sim \frac{c}{\sqrt{i\sigma_P \omega}} \sim \left(\frac{c^2 l^2}{i\sigma_n \omega} \right)^{1/4} \quad \text{and} \quad \zeta_P \sim \frac{\omega \delta_P}{c} \sim l^{1/4} e^{-3i\pi/8}.$$

Note that the Pippard method allows us to define all the dimensional factors correctly, as well as the relation between real and imaginary parts of the impedance.

If for a single crystal metal this situation takes place for a finite interval of the directions of the wave vector $\mathbf{k}$ (or, in other words, for a finite interval of the Euler angles γ), the relation $\zeta \sim l^{1/4}$ remains valid for the polycrystal too. The last is true since when averaging the leading term is defined by the Euler angles corresponding to the maximal values of the local impedance. All the conditions mentioned above are realized for polycrystals composed of the single crystal grains with cubic or cylindrical Fermi surfaces. Consequently, their impedance has to be proportional to $l^{1/4}$.

IV. EFFECTIVE IMPEDANCE IN VICINITY OF ELECTRONIC TOPOLOGICAL TRANSITION

The possibility to observe the effect of a change of topology of the Fermi surface on the properties of electrons was predicted by Lifshitz.[25] The change of topology of the Fermi surface, the electronic topological transition, takes place when the Fermi energy equals one of the critical values ε_c determined by band edges, the Van Hove singularities, local maxima and minima of the function $\varepsilon(\mathbf{p})$. As a consequence of such a change, the properties of a metal determined by the Fermi surface electrons exhibit singularities with different critical exponents. Under the conditions of extremely anomalous skin effect the sensitivity of kinetic properties to the structure of the Fermi surface defines their strong dependence on the parameter $\varepsilon_F - \varepsilon_c$. An attempt to review theoretical papers devoted to the electronic topological transition has been done in Ref. 26.

Two basic types of topological transitions are possible depending on the type of the critical point. They are (1) formation of a new void of the Fermi surface or disappearance of an existing void when the critical point corresponds to a local extremum of the function $\varepsilon(\mathbf{p})$ and (2) creation or disruption of a neck when the critical point corresponds to a conic point of the Fermi surface.

Usually the singularities of the surface impedance in the vicinity of the electronic topological transition are calculated for some chosen orientations of the crystallographic axes with respect to the metal surface (see, for example, Refs. 27, 28). The question we are analyzing in this section is whether the singularities related to the electronic topological transition ''survive'' in polycrystals, which, in effect, are isotropic metals. We will show that the singularities do ''survive,'' and the effective surface impedance of polycrystals exhibits

nontrivial behavior in the vicinity of the electronic topological transition.

Even without calculations it is easy to understand that when a new little void of the Fermi surface appears, the derivative of the effective impedance has a jump. Really, suppose we examine a single crystal metal in the vicinity of a critical point corresponding to an extremum of the function $\varepsilon(\mathbf{p})$. Then the newly appeared void is an ellipsoid. Under the conditions of extremely anomalous skin effect, it is usual to assume that even for electrons of the small void the mean free path $l\to\infty$. Next, the surface impedance is proportional to $S_F^{-1/3}$. After the formation of the new void $S_F=S_0+S_v$, where S_0 is the area of the main part of the Fermi surface and $S_v\sim|\varepsilon_F-\varepsilon_c|$ is the area of the new void. Consequently, in the vicinity of the critical point the impedance $\zeta=\zeta_0+\delta\zeta$, where $\delta\zeta=0$ until the formation of the void, and $\delta\zeta\sim S_v$ is the addition to the impedance caused by the appearance of the new void. Thus, the derivative $\partial\zeta/\partial\varepsilon_F$ has a jump when $\varepsilon_F=\varepsilon_c$.

When calculating the effective impedance, we have to average the impedance of the single crystal with respect to all possible rotations γ. Since the singular addition to the impedance caused by the formation of a new ellipsoidal void has the same sign and is of the same order for all the orientations of the crystallographic axes with respect to the metal surface, the averaging does not change the result qualitatively. The derivative of $\zeta_{\rm ef}$ also has a jump when $\varepsilon_F=\varepsilon_c$. Note, if ε_F is changed by some external effect (e.g., by applying pressure or adding impurities), $\delta\varepsilon_F$ is linear with respect to a small change of the external parameter. Then the derivative of the impedance has a jump with respect to this parameter too.

If the topological transition leads to creation or disruption of a neck of the Fermi surface, the character of the effective impedance singularity cannot be obtained without the calculation. The point is that the orientation of the neck defines ''a preferred direction,'' and the averaging strongly affects the value of the surface impedance. In what follows, we examined a polycrystal composed of the single crystal grains with the Fermi surface of a corrugated cylinder type. This example provides a rather general description of the singularity near the conic point.

As an example of ''an exotic'' topological transition, we analyzed the case of the Fermi surface of the wurzite crystal type for ε_c corresponding to disappearance of the toroidal hole of the Fermi surface and appearance of the new ovaloid void (see Sec. IV B).

A. Fermi surface of corrugated cylinder type

Let the polycrystal be composed of single crystal grains whose Fermi surface with regard to the crystallographic axes is defined by the equation

$$\varepsilon_F=\frac{p_\perp^2}{2m_\perp}+\varepsilon_c\cos\frac{\pi p_z}{p_m},\quad -p_m<p_z<p_m. \tag{33}$$

The topology of the Fermi surface changes at the point $p_z=0$ when $\varepsilon_F=\varepsilon_c$. Namely, (1) if $\varepsilon_F<\varepsilon_c$, the Fermi surface is a closed surface [in each Brillouin zone there are two separated parts belonging to two different closed surfaces, Fig. 2(a)], (2) if $\varepsilon_F=\varepsilon_c$, the Fermi surface has a conic point for $\mathbf{p}=0$, and a neck is formed [see Fig. 2(b)], and (3) if $\varepsilon_F>\varepsilon_c$, the Fermi surface is an open one [see Fig. 2(c)].

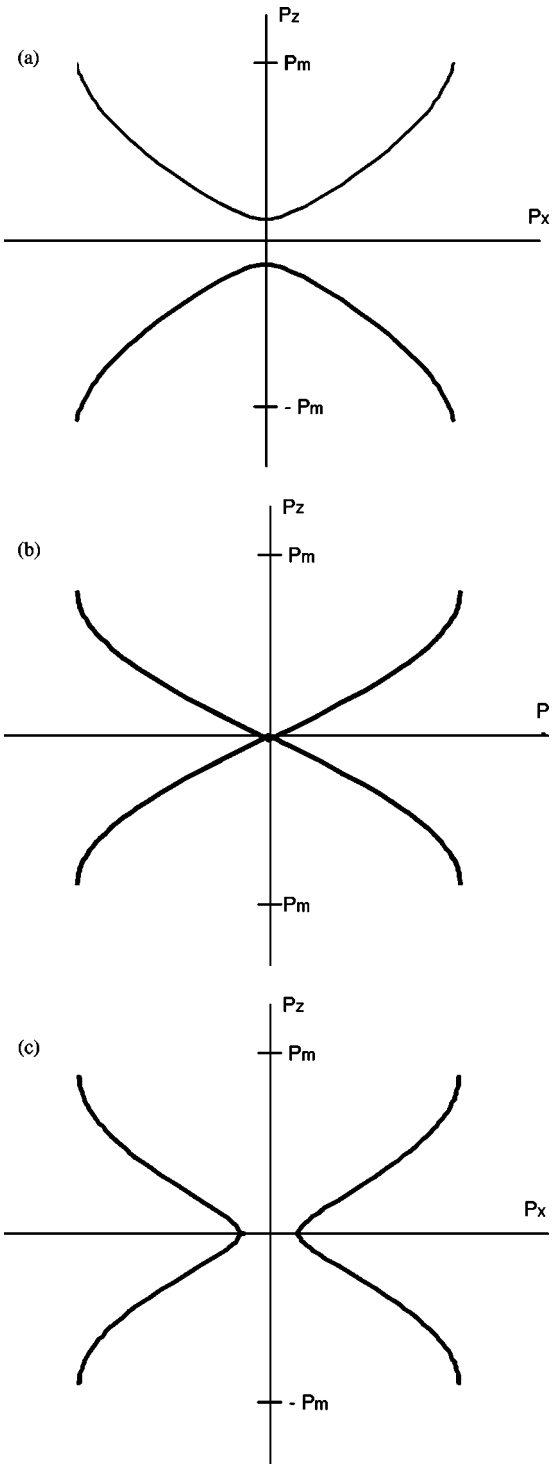

FIG. 2. The cross section of the Fermi surface of a corrugated cylinder type: (a) $\varepsilon_F<\varepsilon_c$, the Fermi surface is a closed surface; (b) $\varepsilon_F=\varepsilon_c$, the Fermi surface has a conic point; (c) $\varepsilon_F>\varepsilon_c$, the Fermi surface is an open surface.

We set

$$\varepsilon_F/\varepsilon_c = 1+\delta\varepsilon, \tag{34}$$

and calculated the effective impedance for $|\delta\varepsilon| \ll 1$. Since the area of the Fermi surface S_F varies under the variation of the Fermi energy ε_F, it is not convenient to use ζ_a defined by Eq. (9) as the characteristic value of the surface impedance. We introduced new characteristics of the Fermi surface independent of ε_F:

$$p_c = \frac{m_\perp \varepsilon c}{p_m}; \quad S_c = 4\pi p_c^2; \quad \mu = \pi^2 \frac{m_\perp \varepsilon c}{p_m^2}. \tag{35}$$

Note, the parameter μ defines the local geometry of the Fermi surface in the vicinity of the conic point: $\mu = m_\perp / m_z^{\mathrm{ef}}(\mathbf{p}=0)$, where $m_z^{\mathrm{ef}}(\mathbf{p}) = \partial^2\varepsilon(\mathbf{p})/\partial p_z^2$ is one of the elements of the effective masses tensor. At the point $\mathbf{p}=0$ we have $m_z^{\mathrm{ef}}(\mathbf{p}=0) = p_m^2/\pi^2\varepsilon_c$.

We used Eqs. (16) and (17) to calculate the effective impedance. By analogy with Eq. (9) we introduced

$$\zeta_c = \frac{2(1-i\sqrt{3})}{3\sqrt{3}}\left(\frac{\omega\delta_c}{c}\right), \quad \delta_c = \left(\frac{4\pi c^2\hbar^3}{\omega e^2 S_c}\right)^{1/3} \tag{36a}$$

(ζ_c did not depend on ε_F) and wrote Eq. (17) in the form

$$\zeta_{\mathrm{ef}}^{(c)} = \zeta_c Z(\delta\varepsilon;\mu). \tag{36b}$$

Next, instead of the Euler angle θ_k we introduced $w = \tan^2\theta_k/\mu$ and substituted $x = p_\perp/\pi p_c$ for $p_\perp$ in Eqs. (16). The obtained expression for the function $Z(\delta\varepsilon;\mu)$ was

$$Z(\delta\varepsilon;\mu) = \frac{\mu}{24\pi^{1/3}}\int_0^\infty \frac{[\tilde{S}_1^{-1/3} + \tilde{S}_2^{-1/3}]}{(1+\mu w)^{3/2}} dw, \tag{36c}$$

$$\tilde{S}_1(w;\mu,\delta\varepsilon) = \frac{\sqrt{1+w\mu}}{w\mu}\int x\Phi(x;w;\mu,\delta\varepsilon)dx;$$

$$\tilde{S}_2(w;\mu,\delta\varepsilon) = \frac{(1+w\mu)^{3/2}}{w\mu}\int \frac{x\,dx}{\Phi(x;w;\mu,\delta\varepsilon)},$$

$$\Phi(x;w;\mu,\delta\varepsilon) = \sqrt{\frac{\mu w x^2}{1-(1+\delta\varepsilon-\mu x^2/2)^2} - 1}. \tag{36d}$$

The requirement for the radicand of Eq. (36d) to be positive combined with inequalities defining the intervals of x variation on the Fermi surface gave the domain of integration.

Let $S_{1(2)}^{(0)}$ be the functions $\tilde{S}_{1(2)}$ for $\delta\varepsilon = 0$ (the Fermi energy corresponds to the conic point). Let $\zeta_{\mathrm{ef}}^{(0)}$ be the effective impedance relevant to this Fermi energy. With regard to Eqs. (36) we have

$$\zeta_{\mathrm{ef}}^{(0)} = \zeta_c Z_0(\mu); \quad Z_0(\mu) = Z(\delta\varepsilon = 0;\mu). \tag{37}$$

The function $Z_0(\mu)$ is presented in Fig. 3.

Let $\delta\zeta_{\mathrm{ef}}^{(c)}$ be $\delta\zeta_{\mathrm{ef}}^{(c)}(\delta\varepsilon) = \zeta_{\mathrm{ef}}^{(c)}(\delta\varepsilon) - \zeta_{\mathrm{ef}}^{(0)}$. If $|\delta\varepsilon| \ll 1$, with regard to Eq. (36c) the leading term of the expression for $\delta\zeta_{\mathrm{ef}}^{(c)}$ is

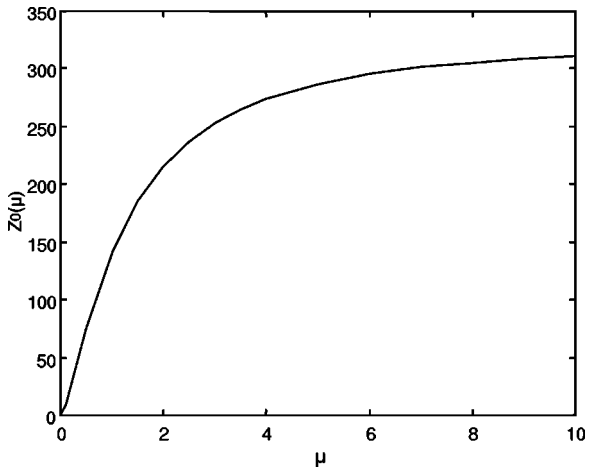

FIG. 3. The function $Z = Z_0(\mu)$ defining the effective impedance when the Fermi surface (33) has the conic point.

$$\delta\zeta_{\mathrm{ef}}^{(c)}(\delta\varepsilon) = \frac{\zeta_c\mu}{6(4\pi)^{1/3}}\int_0^\infty \frac{dw}{(1+\mu w)^{3/2}}\left[\frac{\Delta\tilde{S}_1}{[S_1^{(0)}]^{4/3}} + \frac{\Delta\tilde{S}_2}{[S_2^{(0)}]^{4/3}}\right], \tag{38}$$

where $\Delta\tilde{S}_\alpha = S_\alpha^{(0)}(w;\mu) - \tilde{S}_\alpha(w;\mu,\delta\varepsilon)$.

Below we present the results obtained when calculating $\delta\zeta_{\mathrm{ef}}^{(c)}(\delta\varepsilon)$ for $\delta\varepsilon < 0$ and $\delta\varepsilon > 0$. The details of the calculation are straightforward, but rather lengthy and tedious. In Appendix B we outline the main steps of the calculation. Here we would like to note only, that in both cases the main contribution to $\delta\zeta_{\mathrm{ef}}^{(c)}$ arises from the grains whose orientations are defined by inequality $w = \tan^2\theta_k/\mu > 1$.

So, in the vicinity of the critical point ($|\delta\varepsilon| \ll 1$) our final result for $\delta\zeta_{\mathrm{ef}}^{(c)}$ is

$$\delta\zeta_{\mathrm{ef}}^{(c)} \approx -(\mathrm{sign}\,\delta\varepsilon)\frac{\zeta_c}{3}\left(\frac{\mu}{2\pi}\right)^{5/3}\frac{\alpha^{(\pm)}}{(1+\mu)^2}(|\delta\varepsilon|/2)^{3/4}\ln|\delta\varepsilon|, \tag{39a}$$

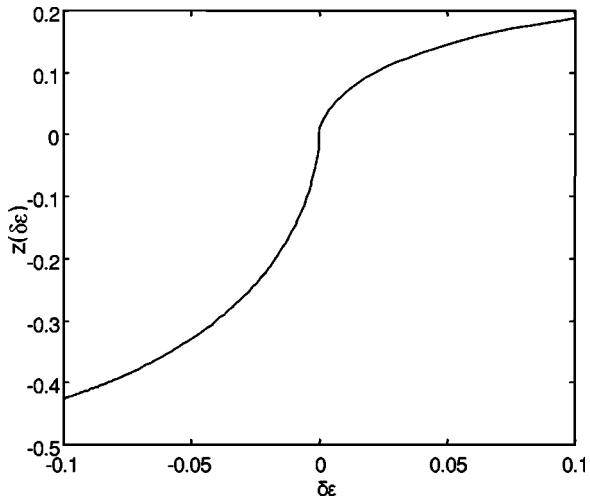

FIG. 4. The singularity of the effective impedance in the vicinity of the electronic topological transition for the case of the neck formation: $z(\delta\varepsilon) = 3\delta\zeta_{\mathrm{ef}}^{(c)}(\delta\varepsilon)(1+\mu)^2(2\pi/\mu)^{5/3}/\zeta_c$.

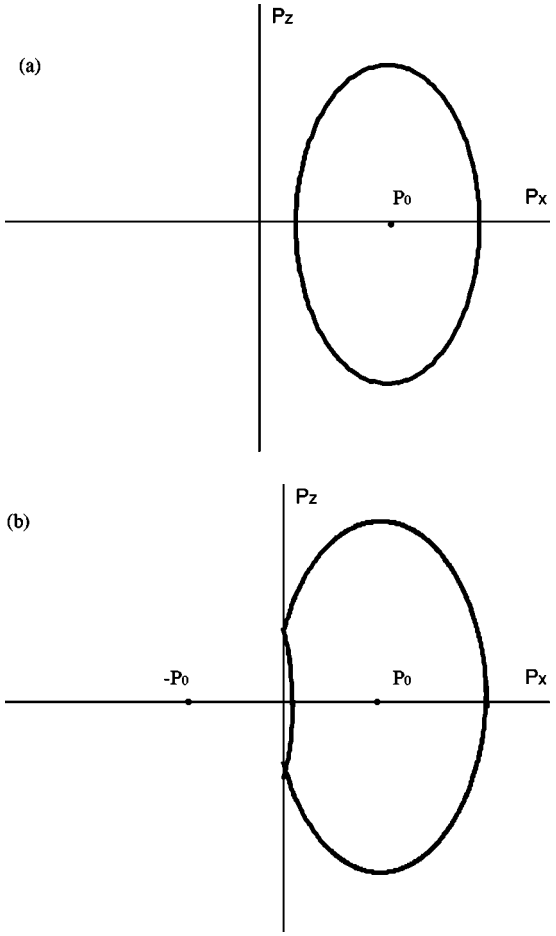

FIG. 5. The equienergy surfaces (40) are obtained by rotation about the axis p_z of the curves shown in (a) for the energies $0<\varepsilon<\varepsilon_c^+$ and (b) for the energies $\varepsilon>\varepsilon_c^+$.

$$\alpha^{(-)}=\int_0^1\frac{(1+x^4)dx}{\sqrt{1-x^4}},\quad \alpha^{(+)}=\int_0^1\frac{(1-x^4)dx}{\sqrt{1+x^4}};\quad (39b)$$

$\alpha^{(-)}\approx 1.75$ corresponds to $\delta\varepsilon<0$, and $\alpha^{(+)}\approx 0.77$ corresponds to $\delta\varepsilon>0$.

These equations describe the singularity of the effective impedance of polycrystals in the vicinity of the electronic topological transition when the Fermi surface passes through the conic point (Fig. 4). We would like to note that, first, this singularity is stronger than when a new void appears: at the conic point the derivative $\partial\zeta_{\rm ef}^{(c)}/\partial\varepsilon_F$ has the infinitely large jump. Secondly, since the expression for $\delta\zeta_{\rm ef}^{(c)}$ depends on the characteristics of the Fermi surface only through the parameter μ, only the local geometry of the Fermi surface in the vicinity of the conic point affects the singularity of the effective impedance [according to the definition (35), μ is the ratio of the effective masses at the point $\mathbf{p}=0$]. This allows us to think that Eqs. (39) are relevant to the general case of creation/disruption of the neck of the Fermi surface in polycrystalline metals.

B. Fermi surface of wurzite type crystals

Let the polycrystal be composed of single crystal grains with an energy spectrum of wurzite type crystals.[19,26] The dispersion relation for such crystals written down with respect to the crystallographic coordinate system is

$$\varepsilon^{\pm}(\mathbf{p})=\frac{1}{2m_\perp}(p_\perp\pm p_0)^2+\frac{1}{2m_z}p_z^2,\qquad (40)$$

where the effective masses $m_\perp$ and m_z are positive.

There are two critical energies $\varepsilon_c^{\pm}$ corresponding to the change of topology of the equienergy surface (40). The first critical energy ε_c^- (we set $\varepsilon_c^-=0$) corresponds to the bottom of the conduction band. Here a new void of the equienergy surface related to minus sign in Eq. (40) appears. When $\varepsilon_F=\varepsilon_c^-$, the critical points $p_\perp=p_0$ form a circle in the momentum space. If $0<\varepsilon<\varepsilon_c^+=p_0^2/2m_\perp$, the equienergy surfaces are toroids with elliptical crossection in the planes containing the axis p_z [Fig. 5(a)]. When the energy equals to the critical value ε_c^+, the hole in the toroid disappears and a new void of ovaloid shape related to plus sign in Eq. (40) appears [Fig. 5(b)] at the point $p_\perp=p_z=0$. Thus, the point $p_\perp=p_z=0$ is an isolated critical point.

For the Fermi energies from the interval $0<\varepsilon_F<\varepsilon_c^+$ we calculated $\zeta_{\rm ef}^w=\zeta_{\rm ef}^{(<)}$ as a function of $\varepsilon_F/\varepsilon_c^+$. For $\varepsilon_F>\varepsilon_c^+$ we wrote down the value of the effective impedance $\zeta_{\rm ef}^w=\zeta_{\rm ef}^{(>)}$ as a sum

$$\zeta_{\rm ef}^{(>)}(\varepsilon_F/\varepsilon_c^+)=\zeta_{\rm ef}^{(<)}(\varepsilon_F/\varepsilon_c^+)+\Delta\zeta.\qquad (41)$$

Here $\zeta_{\rm ef}^{(<)}(\varepsilon_F/\varepsilon_c^+)$ is the extension of the function $\zeta_{\rm ef}^{(<)}$ to the region $\varepsilon_F/\varepsilon_c^+>1$, and $\Delta\zeta$ describes the singularity of the effective impedance in the vicinity of the topological transition related to the critical energy ε_c^+.

We performed the calculation with the aid of Eqs. (16),(17). Some main interim formulas are presented in Appendix C. As in the previous subsection, it is reasonable to introduce a characteristic impedance ζ_w independent of the Fermi energy. With regard to the equation of the Fermi surface (40) and Eq. (9) we set

$$\zeta_w=\frac{2(1-i\sqrt{3})}{3\sqrt{3}}\left(\frac{\omega\delta_w}{c}\right),\quad \delta_w=\left(\frac{\pi c^2\hbar^3}{\omega e^2 m_\perp\varepsilon_c^+}\right)^{1/3}.\quad (42)$$

The direct calculations showed that for $0<\varepsilon_F<\varepsilon_c^+$ the effective impedance was

$$\zeta_{\rm ef}^{(<)}(\varepsilon_F/\varepsilon_c^+)=\zeta_w\left(\frac{\varepsilon_c^+}{\varepsilon_F}\right)^{1/6}B\left(\frac{m_z}{m_\perp}\right).\qquad (43a)$$

The function $B(z)$ is defined by Eqs. (C2) of Appendix C. For $z\ll 1$ and $z\gg 1$ we have

$$B(z)\approx\frac{5}{16}\left(\frac{4}{\pi z}\right)^{1/3}\ \text{if}\ z\ll 1;\quad B(z)\approx\frac{\pi}{8}\frac{z^{1/6}}{\ln z}\ \text{if}\ z\gg 1.\qquad (43b)$$

According to Eq. (43a), when the Fermi energy is near the bottom of the band ($\varepsilon_F\ll\varepsilon_c^+$) the effective impedance has the singularity $\zeta_{\rm ef}^{(<)}\sim\zeta_w(\varepsilon_c^+/\varepsilon_F)^{-1/6}$. In this case the Fermi surface (40) contracts to a circumference $p_\perp=p_0$; $p_z=0$. As a result, the conductivity is unusually small and the imped-

ance is extremely large. Next, the effective impedance increases significantly when toroids are strongly flattened ($m_z/m_\perp \ll 1$) or strongly elongated ($m_z/m_\perp \gg 1$). (Compare with the cases of strongly flattened and strongly elongated ellipsoids discussed in Sec. III A.) Generally, it can be stated that the surface impedance increases significantly, when ''the dimension'' of the Fermi surface decreases.

When $\varepsilon_F > \varepsilon_c^+$, the Fermi surface (40) consists of two parts: the external one is a part of the toroid $\varepsilon_F = \varepsilon^-(\mathbf{p})$; the internal one is a part of the ovaloid $\varepsilon_F = \varepsilon^+(\mathbf{p})$. The straightforward calculation of the function $\Delta\zeta$ [see Eq. (41)] showed that near the point of the topological transition, when $0 < \delta\varepsilon = (\varepsilon_F - \varepsilon_c^+)/\varepsilon_c^+ \ll 1$, the correction to the impedance was

$$\Delta\zeta = -\zeta_w \delta\varepsilon^{3/2} C\left(\frac{m_3}{m_\perp}\right), \tag{44a}$$

where the function $C(z)$ is defined by Eqs. (C3) of Appendix C. For $z \ll 1$ and $z \gg 1$ we had

$$C(z) \approx \frac{1}{36\sqrt{\pi} z^{5/6}} \left(\frac{1}{2\pi}\right)^{1/3} \frac{\Gamma(1/6)}{\Gamma(2/3)} \quad \text{if} \quad z \ll 1;$$

$$C(z) \approx \frac{1}{120 z^{1/6}} \quad \text{if} \quad z \gg 1, \tag{44b}$$

$\Gamma(x)$ is the gamma function. We see the singularity related to the new void formation at the isolated critical point [see Eq. (44a)], is weaker than in the case of a neck formation [see Eqs. (39)]. It is also weaker than in the case of the new void appearance in the vicinity of an extremum of the function $\varepsilon(\mathbf{p})$.

V. CONCLUSIONS

The calculation of the surface impedance of polycrystalline metals is a logical result of the development of electron theory of metals. The possibility to calculate the surface resistance of a polycrystalline metal with high accuracy (in fact, exactly) when the local impedance (the Lentovich) boundary conditions are valid,[11,12] was a stimulus to investigate all the kinds of different physically meaningful situations. Anomalous skin effect is one of these situations. The present analysis relating to extremely anomalous skin effect, together with Refs. 8–12, where the cases of normal skin effect and the infrared spectrum region (see Ref. 9) were examined, completes the theory of skin effect in polycrystals. In the intermediate case, when δ is of the order of l, an analytic expression for the impedance of a single crystal metal (the starting point of our calculation) can be obtained only after rather significant simplifications (see, for example, Ref. 29). The obtained results are applicable in all the cases when the surface resistance is of interest.

Suppose the impedance of an individual single crystal grain is its phenomenological characteristic corresponding to a flat metal-vacuum interface, then Eq. (3) must be considered as the basic formula of the theory. In contrast to other effective characteristics calculated with the aid of the method of Lifshitz and Rosenzweig,[1] the spatial correlators of the local impedance do not enter the expression for the effective impedance. Taking account of these correlators falls outside the limits of the accuracy of the local impedance boundary conditions. This allows us to consider Eq. (3) as an exact formula.

When under the conditions of extremely anomalous skin effect the generally accepted approximation (11) for the conductivity $\sigma_{ik}(\mathbf{k})$ is valid for all the directions of the wave vector $\mathbf{k}$, Eq. (15) solves the problem of the effective impedance calculation. Then the obtained results do not change qualitatively the concept of the polycrystalline metal being in effect an isotropic metal. In this case Eq. (18) allows us to calculate the area $S_F^{(a)}$ of the effective spherical surface defined with regard to anomalous skin effect correctly.

Often when polycrystals are examined, measurements of the impedance under the conditions of extremely anomalous skin effect are used to estimate the area of the Fermi surface. With regard to the measurement of the specific resistance $\rho = 1/\sigma$ the obtained result is used to calculate the electron mean free path. Of course, this method can be used, if the anisotropy of the single crystal grains is small. However, if the anisotropy is strong, the results of the measurements must be handled with care. First, our results show that the calculated area $S_F^{(a)}$ is not the real area of the Fermi surface: the numerical factor in Eq. (18) can significantly differ from unity. Next, the effective static conductivity of a strongly anisotropic polycrystal does not equal to the static conductivity, averaged over all possible rotations of the grains. The difference can be very big (see Ref. 30). Then $S_F^{(s)}$ that enters the equation for the static conductivity of the polycrystal is an effective area defined with regard to the static conductivity. Of course, $S_F^{(s)} \neq S_F^{(a)}$, and this difference has to be taken into account when estimating the electron mean free path.

When the Fermi surface is an axially symmetric surface, the expression for the effective impedance, Eqs. (16) and (17), is much simpler. However, the Fermi surfaces of the majority of real metals are extremely complex. They have many voids of different shapes and symmetry. If one of the voids is axially symmetric, but not all the others, Eqs. (16) and (17) are inapplicable. We can use these equations only if the Fermi surface is axially symmetric as a whole, or if the leading terms in the expression (11b) for elements of the tensor $\hat{S}$ are defined by an axially symmetric void.

When calculating the effective impedance for some different model Fermi surfaces (Sec. III), several problems were the object of our analysis. First of all, an ellipsoidal Fermi surface is the first necessary step, when after the analysis of an isotropic conductor (the conductor with the spherical Fermi surface), we turn to the case of real anisotropic polycrystals. On the other hand the results of Sec. III A also can be applied to bismuth type semimetals and some degenerate semiconductors. In this case, however, these results have to be generalized, since as a rule the Fermi surfaces of semimetals and degenerate semiconductors are the sets of ellipsoids. The cases of extremely anisotropic ellipsoids, in addition to being an illustration of the significant change of the effective area of the Fermi surface [see Eqs. (23)], can be

helpful when low-dimensional systems are analyzed: strongly flattened ellipsoids ($\mu \ll 1$) are relevant for the description of quasi-one-dimensional conductors; strongly elongated ellipsoids ($\mu \gg 1$) are relevant for the description of quasi-two-dimensional conductors.

The analysis of metals with cylindrical (Sec. III B) and cubic (Sec. III C) Fermi surfaces shows that the effective impedance of polycrystals can differ from the impedance of an isotropic metal *qualitatively*. By a qualitative difference we mean the dependence of ζ_{ef} on the mean free path l under the conditions of extremely anomalous skin effect and the unusual relation between its imaginary and real parts [see Eqs. (28) and (31)]. On the other hand, the results of Sec. III can be used as the first approximation under the description of real polycrystals. In particular, the Fermi surfaces of quasi-two-dimensional metals are slightly corrugated cylinders. Apparently, there are metals with a nearly cubic main void of the Fermi surface (see, for example, Ref. 23). By a main void we mean the one where electrons providing the conductivity of the metal are found.

One of the most important phenomena related to the geometry of the Fermi surface is the electronic topological transition.[25] Extremely anomalous skin effect is one of phenomena where the influence of the topological transition manifests itself clearly. Our analysis shows that polycrystals also have singularities of the effective impedance due to the topological transition (the singularities ''survive'' in polycrystals). When in the vicinity of the critical point the impedance of the single crystal metal is not very sensitive to the orientation of the crystallographic axes with respect to the metal surface, the effective impedance of the polycrystal has the singularity of the same kind. If the impedance of the single crystal metal depends on the orientation of the crystallographic axes essentially (for example, when a neck of the Fermi surface is formed), the character of the singularity can change [see Eqs. (39)].

One of the methods allowing to observe the topological transition, is applying of external pressure. In this case it must be taken into account that in a polycrystalline sample the stresses are different in different grains and the transition is blurred. It is better to use polycrystals where the inhomogeneity of the stresses is minimal. Maybe the results of Ref. 31 will be useful for the choice of such polycrystals.

The results of Sec. III and IV confirm the following conclusion: if the anisotropy of the Fermi surface is essential, the averaging necessary when calculating the effective impedance of polycrystals does not liquidate the influence of the geometry of the Fermi surface. In other words, it is not sufficient to think about a polycrystal as of a metal with an effective spherical Fermi surface, since in this case, some characteristic features of extremely anomalous skin effect in polycrystals can be missed.

ACKNOWLEDGMENTS

The authors are grateful to Professor A. M. Dykhne for helpful comments during the course of this work. The work of I.M.K. was supported by RBRF Grant No. 99-02-16533.

APPENDIX A

Let the Fermi surface of a single crystal metal be a surface of revolution $\varepsilon_F = \varepsilon(p_\perp, p_3)$. To calculate the functions $S_{1,2}(\gamma)$ defined by Eqs. (13d), we start with the calculation of elements of the tensor $\hat{S}$ [see Eq. (11b)] with respect to the crystallographic axes. We use the polar coordinates $p_\perp, \phi$. Since with regard to our definition of the elements of the rotation matrix $\mathbf{k}^{(\mathrm{cr})} = k(-\sin\theta_k \cos\psi_k, \sin\theta_k \sin\psi_k, \cos\theta_k)$, in Eq. (11b) $\delta(\mathbf{kv}/kv) = (v/v_\perp \sin\theta_k)\delta[v_z \cot\theta_k/v_\perp - \cos(\psi_k + \phi)]$. Then carrying out the integration with respect to the angle ϕ, we obtain the elements of the tensor $\hat{S}^{(\mathrm{cr})}(\gamma)$:

$$S_{11}^{(\mathrm{cr})}(\gamma) = \frac{8}{S_F \sin\theta_k}\{F_1 + \cos 2\psi_k [2\cot^2\theta_k F_2 - F_1]\}; \tag{A1a}$$

$$S_{12}^{(\mathrm{cr})}(\gamma) = -\frac{8\sin 2\psi_k}{S_F \sin\theta_k}[2\cot^2\theta_k F_2 - F_1];$$

$$S_{13}^{(\mathrm{cr})}(\gamma) = \frac{16\cos\psi_k \cot\theta_k}{S_F \sin\theta_k} F_2; \tag{A1b}$$

$$S_{22}^{(\mathrm{cr})}(\gamma) = \frac{8}{S_F \sin\theta_k}\{F_1 - \cos 2\psi_k [2\cot^2\theta_k F_2 - F_1]\}; \tag{A1c}$$

$$S_{23}^{(\mathrm{cr})}(\gamma) = -\frac{16\sin\psi_k \cot\theta_k}{S_F \sin\theta_k} F_2; \quad S_{33}^{(\mathrm{cr})}(\gamma) = \frac{16}{S_F \sin\theta_k} F_2. \tag{A1d}$$

Here the functions $F_1(\theta_k)$ and $F_2(\theta_k)$ are

$$F_1(\theta_k) = \int \frac{v_\perp^2 p_\perp dp_\perp}{v_z \sqrt{v_\perp^2 - v_z^2 \cot^2\theta_k}},$$

$$F_2(\theta_k) = \int \frac{v_z p_\perp dp_\perp}{\sqrt{v_\perp^2 - v_z^2 \cot^2\theta_k}}. \tag{A2}$$

The integration is carried out over the region of the Fermi surface, where $v_z > 0$ and $v_\perp^2 - v_z^2 \cot^2\theta_k > 0$.

We use Eqs. (A1a)–(A1d) and Eq. (A2) to calculate the elements of the tensor $\hat{S}$ with respect to the laboratory coordinate system. With regard to Eq. (12) we obtain

$$S_{11}(\gamma) = \frac{8}{S_F \sin\theta_k}[F(\theta_k) - \cos 2\varphi_k \Phi(\theta_k)];$$

$$S_{22} = \frac{8}{S_F \sin\theta_k}[F(\theta_k) + \cos 2\varphi_k \Phi(\theta_k)]; \tag{A3a}$$

$$S_{12}(\gamma) = -\frac{8\sin 2\varphi_k}{S_F \sin\theta_k}\Phi(\theta_k); \quad S_{i3}(\gamma) = 0; \quad (i = 1,2,3). \tag{A3b}$$

$$F(\theta_k) = F_1(\theta_k) + F_1(\theta_k);$$

$$\Phi(\theta_k)=F_1(\theta_k)-\frac{(1+\cos^2\theta_k)}{\sin^2\theta_k}F_2(\theta_k). \tag{A4}$$

Now it is easy to see that the functions $R(\gamma)$ and $s(\gamma)$ defined by Eq. (13d) and Eq. (14c), respectively, are

$$R(\gamma)=\frac{16}{S_F\sin\theta k}\Phi(\theta_k),\quad s(\gamma)=-\cos 2\varphi_k. \tag{A5}$$

The expressions (16) for the functions $S_{1,2}(\theta_k)$ are the result of substitution of Eqs. (A3) and Eqs. (A5) into Eqs. (13d).

APPENDIX B

Here we present the formulas related to the Fermi surfaces of the corrugated cylinder type (33). With regard to Eqs. (36), first of all we have to calculate the functions $\tilde{S}_{1(2)}$. To specify the domains of integration in Eqs. (36d), we take into account that the radicand of the expression for $\Phi(x;w;\mu,\delta\varepsilon)$ vanishes when $x=x_\pm$,

$$x_\pm^2=\frac{2}{\gamma}[(1-w)+\delta\varepsilon\pm\Delta(w;\delta\varepsilon)];$$

$$\Delta(w;\delta\varepsilon)=\sqrt{(1-w)^2-2\delta\varepsilon w}. \tag{B1a}$$

Since $|\delta\varepsilon|\ll 1$, we set

$$\Delta(w;\delta\varepsilon)=|1-w|-2(\operatorname{sgn}\delta\varepsilon)\,\eta^{(\pm)}(w;|\delta\varepsilon|), \tag{B1b}$$

where the small additions $\eta^{(-)}(w;|\delta\varepsilon|)$ and $\eta^{(+)}(w;|\delta\varepsilon|)$ correspond to $\delta\varepsilon>0$ and $\delta\varepsilon<0$, respectively.

Let us begin with the case $\delta\varepsilon<0$. Here for all w the domain of integration in Eqs. (38d) is $x_+<x<x_m$, where $x_m=\sqrt{2(2-|\delta\varepsilon|)/\mu}$ is the maximal value of $x=p_\perp/\pi p_c$ allowed by the equation of the Fermi surface (33).

With regard to Eq. (B1b) when calculating the functions $\Delta\tilde{S}_\alpha(w;\delta\varepsilon)$, $(\alpha=1,2)$ the regions $w<1$ and $w>1$ have to be examined separately. If $0<w<1$, $\eta^{(-)}(w;|\delta\varepsilon|)\leqslant\sqrt{|\delta\varepsilon|/2}$. When $w>1$, $|\delta\varepsilon|/2\leqslant\eta^{(<)}(w;|\delta\varepsilon|)\leqslant\sqrt{|\delta\varepsilon|/2}$.

We showed that if $0<w<1$, $\Delta\tilde{S}_\alpha(w)\sim\eta^{(-)}$. If $w>1$ up to the leading terms in $\eta^{(-)}$

$$\Delta\tilde{S}_1(w)=-\frac{1}{\mu^2}\sqrt{\frac{1+\mu w}{w}}\sqrt{\frac{w-1}{w}}\eta^{(-)}(w;|\delta\varepsilon|)\times\ln\eta^{(-)}(w;|\delta\varepsilon|), \tag{B2a}$$

$$\Delta\tilde{S}_2(w)=\frac{1}{\mu^2}\left(\frac{1+\mu w}{w}\right)^{3/2}\sqrt{\frac{w}{w-1}}\eta^{(-)}(w;|\delta\varepsilon|)\times\ln\eta^{(-)}(w;|\delta\varepsilon|). \tag{B2b}$$

Consequently, the region $w>1$ provided the main contribution to $\delta\zeta_{\mathrm{ef}}^{(c)}$ when $\delta\varepsilon<0$.

Now we start with the case $\varepsilon_F/\varepsilon_c>1$ that is $\delta\varepsilon>0$. Our analysis showed that here three intervals of w variation, namely $0<w<w_-$, $w_-<w<w_+$ and $w_+<w<\infty$ $(w_\pm=1+\delta\varepsilon\pm\sqrt{\delta\varepsilon(2+\delta\varepsilon)})$, have to be examined separately. Simple algebra allowed to determine three different domains of integration in Eqs. (36d) with regard to the three intervals of w variation. We showed that when $\delta\varepsilon\ll 1$, only w from the interval $w_+<w<\infty$ contributed to the leading term of the expression (38) for $\delta\zeta_{\mathrm{ef}}^{(c)}(\delta\varepsilon)$.

It was found out that for $w>w_+$ the leading terms in the expressions for $\Delta\tilde{S}_{1(2)}(w)$ were given by Eq. (B2a) and Eq. (B2b), respectively, where $\eta^{(+)}(w;\delta\varepsilon)$ was substituted for $\eta^{(-)}(w;|\delta\varepsilon|)$ and the signs changed. In this case the calculation of $\delta\zeta_{\mathrm{ef}}^{(c)}(\delta\varepsilon)$ was reduced to the calculation of the integral (38) over the region $w_+<w<\infty$. The difference in the numerical factors $\alpha^{(-)}$ and $\alpha^{(+)}$ entering Eq. (39a) arose from this last integration.

APPENDIX C

When Eqs. (16),(17) are used to calculate the effective impedance for the energy spectrum of the wurzite type crystals (40), it is convenient to use

$$f(\theta_k)=\frac{\cot\theta_k}{\sqrt{m_z/m_\perp+\cot^2\theta_k}} \tag{C1a}$$

in place of the Euler angle θ_k. Then the averaging in Eq. (17) corresponds to integration with respect to f:

$$\langle\cdots\rangle=\sqrt{\frac{m_z}{m_\perp}}\int_0^1\frac{(\cdots)df}{[1+f^2(m_z/m_\perp-1)]^{3/2}}. \tag{C1b}$$

When $0<\varepsilon_F<\varepsilon_c^+$, the Fermi surface is the toroid $\varepsilon_F=\varepsilon^-(\mathbf{p})$. Our calculation showed that the function $B(z)$ in Eq. (43a) for $\zeta_{\mathrm{ef}}^{(w)}$ was

$$B(z)=\frac{z^{1/3}}{4}\int_0^1\frac{df}{[1+f^2(z-1)]^{5/3}}\times\left\{B_1(f)+\left[\frac{z}{1+f^2(z-1)}\right]^{1/3}B_2(f)\right\} \tag{C2a}$$

and

$$B_1(f)=\left[\frac{E(\sqrt{1-f^2})-f^2K(\sqrt{1-f^2})}{1-f^2}\right]^{-1/3},$$

$$B_2(f)=\left[\frac{K(\sqrt{1-f^2})-E(\sqrt{1-f^2})}{1-f^2}\right]^{-1/3}; \tag{C2b}$$

$K(k)$ and $E(k)$ are full elliptic integrals of the first and the second kind, respectively.

When $\varepsilon_F>\varepsilon_c^+$, the Fermi surface consists of the external toroidal part $[\varepsilon_F=\varepsilon^-(\mathbf{p})]$ and the internal ovaloid part $[\varepsilon_F=\varepsilon^+(\mathbf{p})]$. It is worth to be mentioned, that in this case, in Eqs. (16) not only an additional domain of integration related to the internal part of the Fermi surface appears, but the domain of integration related to the external part of the Fermi surface also changes.

We calculated $\zeta_{\rm ef}^{(>)}(\varepsilon_F/\varepsilon_c^+)$ for an arbitrary value of the parameter $\delta\varepsilon=(\varepsilon_F-\varepsilon_c^+)/\varepsilon_c^+>0$. Near the point of the topological transition, $0<\delta\varepsilon\ll 1$, our result for $\Delta\zeta(\delta\varepsilon)$ was given by Eq. (44a), where the function $C(z)$ was

$$C(z)=\frac{z^{1/3}}{36}\int_0^1\frac{[B_1(f)]^4 df}{[1+f^2(z-1)]^{5/3}\sqrt{1-f^2}} \tag{C3}$$

with the function $B_1(f)$ from Eq. (C2b).

[1] I.M. Lifshitz and L.N. Rosenzweig, Zh. Éksp. Teor. Fiz. **16**, 967 (1946).
[2] I.M. Lifshitz and G.D. Parkhomovskii, Zh. Éksp. Teor. Fiz. **20**, 175 (1950).
[3] I.M. Lifshitz, M.I. Kaganov, and V.M. Tzukernic, *Selected Works of I.M. Lifshitz* (Nauka, Moscow, 1987).
[4] V.I. Tatarskii, Zh. Eksp. Teor. Fiz. **46**, 1399 (1964) [Sov. Phys. JETP **19**, 946 (1964)].
[5] A.M. Dykhne, Zh. Eksp. Teor. Fiz. **59**, 110 (1970) [Sov. Phys. JETP **32**, 63 (1970)].
[6] I.M. Kaganova and A.A. Maradudin, Phys. Scr. **T44**, 104 (1992).
[7] I.M. Kaganova, Phys. Rev. B **51**, 5333 (1995).
[8] I.M. Kaganova and M.I. Kaganov, Phys. Lett. A **173**, 473 (1993).
[9] I.M. Kaganova and M.I. Kaganov, Waves Random Media **3**, 177 (1993).
[10] I.M. Kaganova and M.I. Kaganov, J. Low Temp. Phys. **22**, 712 (1996).
[11] A.M. Dykhne and I.M. Kaganova, Physica A **241**, 154 (1997).
[12] A.M. Dykhne and I.M. Kaganova, Phys. Rep. **288**, 263 (1997).
[13] M.A. Leontovich, *Investigation on Radiowaves Propagation* (Publishing House of the Academy of Science of USSR, Moscow, 1948).
[14] L.D. Landau and E.M. Lifshitz, *Electrodynamics of Continuous Media* (Pergamon, Oxford, 1984).
[15] E.L. Feinbeg, J. Phys. (France) **9**, 1 (1945); **10**, 4 (1946).
[16] L.L. Bonilla and J.B. Keller, J. Mech. Phys. Solids **33**, 241 (1985).
[17] P. Bussemer, K. Hehl, S. Kassam, and M.I. Kaganov, Waves Random Media **2**, 113 (1991).
[18] C. Pecharroman and J.E. Iglesias, Phys. Rev. B **49**, 7137 (1994).
[19] I.M. Lifshitz, M.Ya. Asbel', and M.I. Kaganov, *Electron Theory of Metals* (Consultants Bureau, New York, 1973).
[20] A.P. Cracknell and K.C. Wong, *The Fermi Surface. Its Concept, Determination, and Use in the Physics of Metals* (Clarendon Press, Oxford, 1973).
[21] E.M. Lifshitz and L.P. Pitaevskii, *Physical Kinetics* (Pergamon, Oxford, 1981).
[22] G.Ya. Lyubarskii, *The Application of Group Theory in Physics* (Pergamon Press, Oxford, 1960).
[23] V.I. Nezhankovskii, Pis'ma Zh. Eksp. Teor. Fiz. **51**, 191 (1990) [JETP Lett. **51**, 217 (1990)].
[24] A.B. Pippard, Proc. R. Soc. London, Ser. A **191**, 385 (1947).
[25] I.M. Lifshitz, Zh. Eksp. Teor. Fiz. **38**, 1569 (1960) [Sov. Phys. JETP **11**, 1130 (1960)].
[26] Ya.M. Blanter, M.I. Kaganov, A.V. Pantsulaya, and A.A. Varlamov, Phys. Rep. **245**, 160 (1994).
[27] M.I. Kaganov and P. Kontrares, Zh. Eksp. Teor. Fiz. **106**, 1814 (1994) [JETP **79**, 985 (1994)].
[28] N.A. Zimbovskaya and V.I. Okulov, Fiz. Met. Metalloved. **61**, 230 (1986).
[29] M.I. Kaganov, G.Ya. Lyubarskii, and E. Chervonko, Zh. Eksp. Teor. Fiz. **101**, 1351 (1992) [Sov. Phys. JETP **74**, 725 (1992)].
[30] Yu.A. Dreizin and A.M. Dykhne, Zh. Eksp. Teor. Fiz. **84**, 1756 (1983) [Sov. Phys. JETP **57**, 1024 (1983)].
[31] I.M. Kaganova and A.L. Roitburd, Solid State Phys. **31**, 1 (1989).